

Single-File Diffusion of Colloids in One-Dimensional Channels

Christoph Lutz,^{1,2} Markus Kollmann,³ and Clemens Bechinger¹¹*Physikalisches Institut, Universität Stuttgart, Pfaffenwaldring 57, 70550 Stuttgart, Germany*²*Fachbereich Physik, Universität Konstanz, 78457 Konstanz, Germany*³*Dipartimento di Fisica, Viale delle Scienze, Università di Palermo, 90141 Palermo, Italy*

(Received 8 September 2003; published 8 July 2004)

We study the diffusive behavior of colloidal particles which are confined to one-dimensional channels generated by scanning optical tweezers. At long times t , the mean-square displacement is found to scale as $t^{1/2}$, which is expected for systems where single-file diffusion occurs. In addition, we experimentally obtain the long-time, self-diffusive behavior from the short-time collective density fluctuations of the system as suggested by a recent analytical approach [M. Kollmann, *Phys. Rev. Lett.* **90**, 180602 (2003)].

DOI: 10.1103/PhysRevLett.93.026001

PACS numbers: 83.50.Ha, 82.70.Dd, 83.80.Hj

Single-file diffusion (SFD), prevalent in many physical, chemical, and biological processes, refers to the one-dimensional (1D) motion of interacting particles in pores which are so narrow that the mutual passage of particles is excluded. Since the sequence of particles in such a situation remains unaffected over time t , this leads to strong deviations from normal diffusion. One of the most striking features of SFD is that the mean-square displacement (MSD) $W(t)$ of a tracer particle for t much larger than the direct interaction time τ (i.e., the time a particle needs to move a significant fraction of the mean particle distance) is given by [1–5]

$$\lim_{t \gg \tau} W(t) = F\sqrt{t}, \quad (1)$$

where F is the SFD mobility. While most of the results for SFD are limited to hard-rod systems [6–8], only recently has it been demonstrated by one of us that Eq. (1) remains valid for colloidal and atomic systems with arbitrary interaction potentials, provided the correlation length between the particles is of finite range and collisions are associated with some energy dissipation [9]. In addition, it was shown that the SFD mobility F can be determined by the compressibility and the short-time collective diffusion coefficient of the system. This is an interesting result, because it relates in a unique way a long-time feature, i.e., the SFD mobility to the short-time collective diffusional properties of the system.

Although the asymptotic $t^{1/2}$ behavior of SFD systems was predicted almost 40 years ago, experimental studies of such non-Fickian diffusion processes were lacking for a long time. However, due to recent progress in the synthesis of zeolitic materials which consist of long quasi-cylindrical pores with diameters of several angstroms [10], experimentally accessible SFD systems are now available. By means of pulsed force gradient nuclear magnetic resonance (PFG-NMR) experiments, it was demonstrated that the transport of methane and ethane in such molecular sieves can indeed be described by SFD

[2,3]. Experimental evidence for the occurrence of SFD as provided by different authors, however, remains contradictory [11]. In addition, some of the results obtained with PFG-NMR are not in agreement with recent quasi-elastic neutron scattering studies, which show that both methane and ethane exhibit normal diffusion in AlPO_4 molecular sieves [12]. Several possible reasons have been suggested to account for this discrepancy: First, due to almost inevitable deviations of the real structure in zeolites from the ideal one, the nanopores in the samples are not infinitely long. Additionally, due to possible interactions between molecules in neighboring channels, e.g., due to van der Waals forces, enormous deviations from an ideal $t^{1/2}$ behavior may occur [13,14].

An alternative approach for systematic investigations of SFD is the use of colloidal particles whose dynamical properties are governed by Brownian motion. Owing to the mesoscopic length scales and their (compared to atoms or molecules) rather slow diffusion constants, it is possible to study the trajectories of individual colloidal particles. In view of the above mentioned ambiguities in atomic systems, this is of considerable advantage because direct structural information is provided in colloidal systems. So far, only a few studies with colloidal systems are reported in the literature. The short-time properties of slightly charged silica spheres in 1D channels were investigated by Lin *et al.*, who found for $t \ll \tau$ normal diffusion [15]. At later times the same authors observe a subdiffusive motion, which is explained in terms of hydrodynamic coupling between the particles. Wei *et al.* studied the long-time behavior of systems comprised of super paramagnetic colloids which were confined to topographically channels and indeed found the MSD to scale with $t^{1/2}$ [16]. In these experiments, however, the crossover from normal to SFD diffusion could not be resolved. In addition, a comparison between experimentally obtained SFD mobilities F which characterize the efficiency of particle transport in 1D systems with theoretical values is still lacking.

In this Letter, we report on the study of highly interacting charged colloidal spheres in 1D circular channels. Our data clearly resolve the transition from normal diffusion at short times to the predicted $t^{1/2}$ long-time behavior of the MSD. The channels were — in contrast to previous measurements — created by means of scanning optical tweezers. Because of the absence of lateral confinement walls (as unavoidably present in topographical structures), the particles have a significantly higher mobility. We also compared the measured SFD mobility with the corresponding value as obtained from the initial decay of the dynamic structure factor $S(q, t)$ and find good agreement with recent theoretical predictions [9].

As a colloidal system we used a highly diluted aqueous suspension of sulphate-terminated polystyrene particles of $2.9 \mu\text{m}$ diameter. The experimental setup was composed of a silica glass cuvette with $200 \mu\text{m}$ spacing, which was connected to a standard deionization circuit [17]. Prior to inserting colloidal particles into the cell, the water in the whole circuit was highly deionized (corresponding to an ionic conductivity below $0.07 \mu\text{S}/\text{cm}$). The experiments were performed at $294 \pm 0.5 \text{ K}$. When the cell was disconnected from the circuit, stable conditions during several hours were maintained. The confinement of the particles to 1D channels was achieved with an optical tweezer setup, which provided a stable trapping potential for the colloids [18]. In order to create ring-shaped channel structures, a laser beam ($\lambda = 532 \text{ nm}$) was deflected from a pair of computer-controlled galvanostatic driven mirrors and focused into the sample cell, where the beam created a ring-shaped light pattern. The repetition rate of the circular pattern was about 300 Hz , which is fast enough to provide a quasistatic circular optical trap for the particles [19]. The measured averaged drift rate was about $\pm 2.9 \times 10^{-4} \mu\text{m}/\text{s}$ and independent of the laser scanning direction. This rules out drift effects induced by the scanning laser beam. The laser was circularly polarized by a quarter-wave plate, which reduced any residual inhomogeneity of the laser intensity along the circular path to about 3%. Since the half width of the light pattern perpendicular to the scanning direction corresponded to about one particle diameter, the scanned-laser optical trap provided an effective 1D potential for the colloids where mutual passage of particles is excluded (under the experimental conditions, radial particle fluctuations were less than one particle diameter). Based on Ref. [20], we estimated the effective changes in the lateral particle interaction between neighboring particles due to the pushing light forces. A rough calculation yields that this effect can be ignored in comparison to the static pair potential. The depth of the light potential was on the order of $10k_B T$ (corresponding to a laser power of $10\text{--}20 \text{ mW}$ inside the cell), which is sufficient to impede colloidal particles from escaping out of the trap during our measuring times. Density dependent measurements were performed by variation

of the radius R of the circular optical trap ($35 < R < 49 \mu\text{m}$) and the number of particles N ($22 < N < 45$).

Because the laser tweezer was incident perpendicular from above, the particles were also subjected to vertical light forces which pushed them toward the negatively charged silica substrate. Therefore, the system was effectively confined to two dimensions. The particle center positions were analyzed during the experiments online with an imaging processing software.

A typical real-space configuration of 45 particles in a circular optical trap with $R = 42 \mu\text{m}$ diameter is shown in Fig. 1. From the particle trajectories which were recorded up to several hours, we calculated $W(t) = \frac{1}{2N} \sum_i \langle [x_i(t + t') - x_i(t')]^2 \rangle$, where x corresponds to the angular position multiplied by R , i denotes the particle index, and the brackets indicate averaging over all time steps. The results are shown as symbols in Fig. 2 for different particle number densities [$\rho = 0.103 \mu\text{m}^{-1}$ (Δ), $0.119 \mu\text{m}^{-1}$ (\square), $0.168 \mu\text{m}^{-1}$ (∇), $0.185 \mu\text{m}^{-1}$ (\circ), and $0.203 \mu\text{m}^{-1}$ (\boxplus)] in a log-log representation. At sufficiently short times ($t < 10 \text{ s}$) where the individual particles do not “feel” the presence of other particles by direct interactions, normal diffusion occurs and the mean-square displacement is found to be $W(t) \propto t$ (see dashed line). This behavior is in good agreement with Lin *et al.*, who also studied the short-time diffusional motion of colloidal particles in 1D channels [15]. In the case of topographically created 1D channels, the diffusion coefficient is strongly influenced by the walls and the local particle density ρ . This dependence on hydrodynamic boundary conditions is significantly reduced in our system, as lateral walls are absent and only the substrate determines the free diffusion constant. With increasing

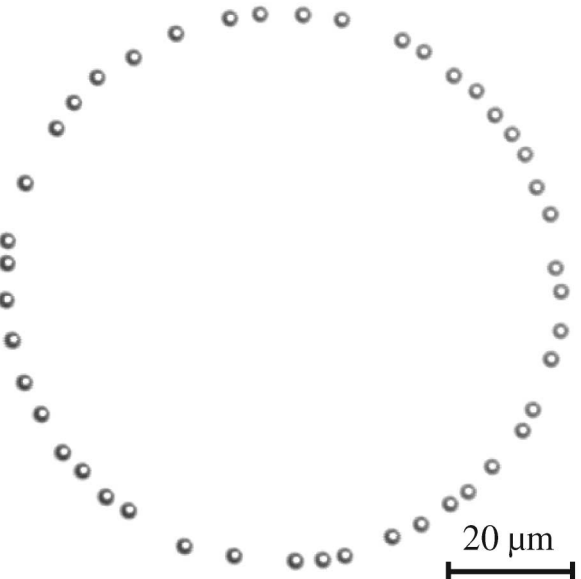


FIG. 1. Image of colloidal particles which are trapped by a scanning laser beam to a circular optical trap (the trap itself is not imaged but was blocked with appropriate optical filters).

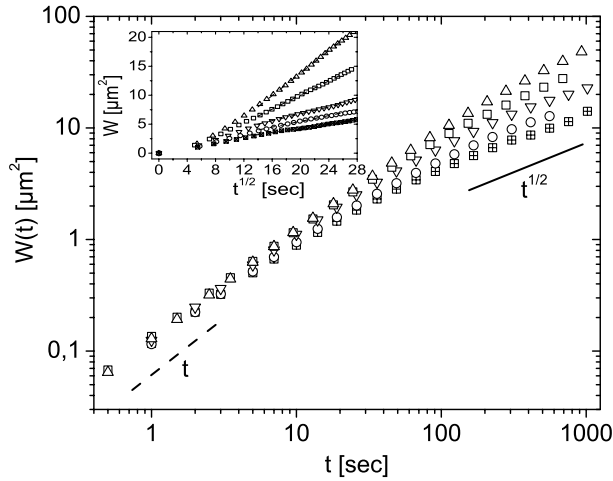


FIG. 2. log-log plot of W for $\rho = 0.103 \mu\text{m}^{-1}$ (Δ), $0.119 \mu\text{m}^{-1}$ (\square), $0.168 \mu\text{m}^{-1}$ (∇), $0.185 \mu\text{m}^{-1}$ (\circ), and $0.203 \mu\text{m}^{-1}$ (\boxplus). The dotted line with slope 1 illustrates normal diffusion and the solid line with slope 0.5 describes SFD. The inset shows the same data plotted as W vs \sqrt{t} , with the solid lines corresponding to fits to Eq. (1).

time the presence of adjacent particles becomes more and more important until eventually a crossover to a $t^{1/2}$ behavior occurs (solid line in Fig. 2). In contrast to earlier experiments [16], here both regimes are clearly resolved for the first time. It is clearly seen that the crossover from normal to SFD occurs at earlier times as ρ is increased. This is due to the fact that, with increasing ρ , the clearance between adjacent particles is smaller and therefore direct particle-particle interactions occur at shorter times.

To obtain the SFD mobility F for our data, we first plotted W vs $t^{1/2}$ and applied a fit of Eq. (1) (see inset in Fig. 2). As the lower bound for the fitting range we have chosen the direct interaction time of the particles, which is on the order of 200 s. It can be clearly seen that above this time, all curves show a linear behavior. The obtained values for F are plotted in Fig. 3 as solid squares and show that F decreases monotonically with ρ . Such a monotonic behavior of F has also been observed for the diffusion of CF_4 in AlPO_4 zeolites at low temperatures [2] and is in qualitative agreement with an analytical expression derived for hard rods [5]. It is important to realize that in the case of normal diffusion, the diffusion coefficient will saturate at small ρ , while in the case of SFD, even at very low ρ , no saturation of F occurs. This emphasizes that particle-particle interactions are the limiting factor for SFD [2]. As mentioned above, theoretical predictions for the SFD mobility F were for a long time available only for hard-rod systems where analytical expressions for the limit of small-rod densities were derived [11]. Very recently, however, a general theory of SFD for systems of identical Brownian particles with arbitrarily interaction potentials was developed. It has been shown [9] that the long-time behavior of the MSD for $q \ll a^{-1}$

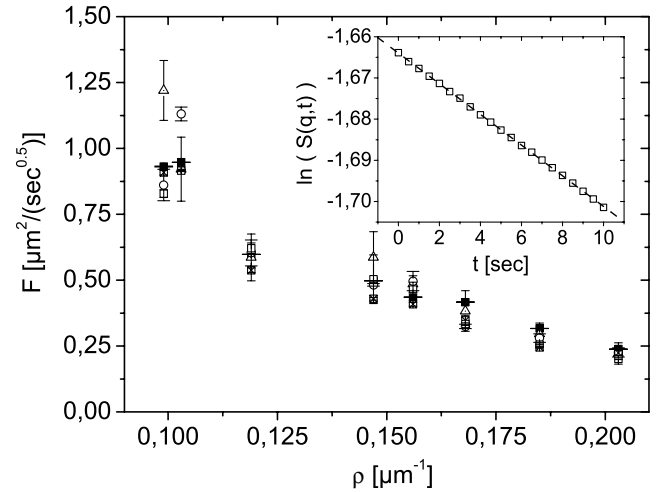


FIG. 3. Comparison of SFD mobilities F obtained with different methods as a function of the particle number density ρ : F derived from fitting the MSD in Fig. 2 at long times (\blacksquare), F taken from the decay of the dynamic structure factor according to Eq. (2) for $q = 3q_{\min}$ (Δ), $q = 4q_{\min}$ (\circ), $q = 5q_{\min}$ (\boxtimes), and $q = 6q_{\min}$ (\square). The inset shows the decay of $S(q, t)$ for $q = 4q_{\min}$, which follows an exponential function (solid line).

and is given by

$$\lim_{t \gg \tau} W(t) = \frac{S(q, t=0)}{\rho} \sqrt{\frac{D^{\text{eff}}(q)t}{\pi}}. \quad (2)$$

Here $S(q, t=0)$ is the static structure factor and $D^{\text{eff}}(q)$ is the collective diffusion coefficient, which can be experimentally determined by a short-time measurement of the dynamic structure factor $S(q, t) = \frac{1}{N} \sum_{i,j=1}^N \langle \exp\{iq[r_i(0) - r_j(t)]\} \rangle$. For small wave vectors $q \ll a^{-1}$ and $t < \tau$, with a being the mean particle distance and hydrodynamic interactions (HI) neglected or treated in a pairwise fashion, $S(q, t)$ is given by $S(q, t) = S(q, 0) \exp[-q^2 D^{\text{eff}}(q)t]$ [21]. Since $S(q, t=0)$ and $D_{\text{eff}}(q)$ can be experimentally determined from a short-time measurement, Eq. (2) predicts the long-time behavior of the MSD to be obtained already at short times, i.e., significantly earlier than the crossover time from normal to SFD diffusion suggests (cf. Fig. 2). To understand this—at first glance surprising—result, one has to realize that, owing to the absence of mutual particle passages during SFD, the motion of a density wave with $q \ll a^{-1}$ is reflected by the trajectory of every individual particle. In contrast, when particles can pass each other, i.e., during normal diffusion, the motion of an arbitrarily chosen particle is decoupled from the collective motion of the system and Eq. (2) does not apply.

From the particle trajectories we determined the density dependent $S(q, t)$ for $t < 10$ s, which is shown exemplarily for $q = 4q_{\min}$ with $q_{\min} = \frac{1}{R}$ in the inset in Fig. 3 (owing to the finiteness of the system, we are limited to wave vectors $q > q_{\min} = 1/R$). From the vertical axis intercept and the slope we obtain $S(q, t=0)$ and

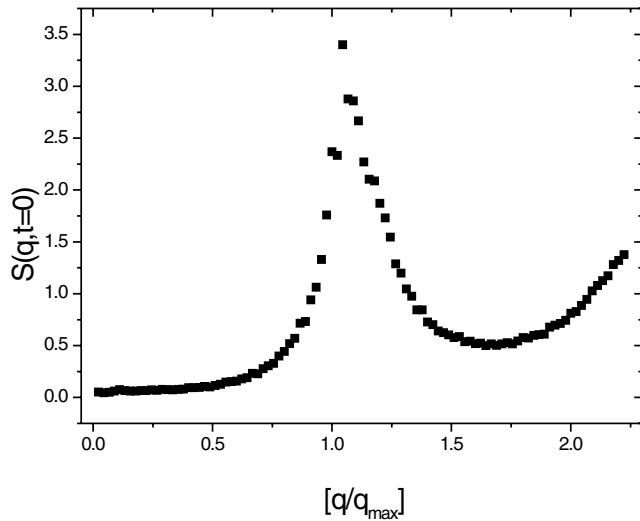


FIG. 4. Real part of static structure factor $S(q, t = 0)$ for $\rho = 0.203 \mu\text{m}^{-1}$ ($q_{\text{max}} = 2\pi/a$).

$D^{\text{eff}}(q)$, which allows us to calculate $F = S(q, 0)/\rho\sqrt{D^{\text{eff}}(q)/\pi}$ according to Eq. (2). The results are plotted for $3q_{\text{min}}$, $4q_{\text{min}}$, $5q_{\text{min}}$, and $6q_{\text{min}}$ as open symbols in Fig. 3 and show good agreement with the previously calculated values from the long-time MSD measurements [the deviations at small ρ are probably due to the breakdown of the long wave limit $q \ll a^{-1}$ of Eq. (2)]. This result demonstrates the validity of Eq. (2) even in the case of finite systems as used here. This indicates that, owing to the short-ranged electrostatic particle pair potential, particle correlations within the ring-shaped channels decay on a length scale much shorter than the perimeter of the system [22]. This is also seen by the behavior of the static structure factor, which is plotted in Fig. 4. The rather horizontal slope for $q \rightarrow 0$ resembles the behavior of an infinite system and thus justifies *a posteriori* application of Eq. (2). In addition, this suggests that Eq. (2) is also valid in finite biological systems where the screening length is very small.

It should be emphasized that Eq. (2) is very general and applies for any other stochastic process in a many-particle system as far as it remains translational invariant in space and time. In the absence of HI (and $q \rightarrow 0$), Eq. (2) simplifies to $\lim_{t \gg \tau} W(t) = \frac{1}{\rho} \sqrt{S(q)Dt/\pi}$, with D the diffusion constant of a single particle, i.e., $D = \text{const}$.

In summary, we have investigated the diffusion of colloidal particles in an optically created circular trap where the particles undergo SFD. Owing to the lack of sticking hydrodynamic conditions at the lateral confinement walls, this allows us to observe the transition from normal to SFD diffusion. In addition, we compare the SFD mobility F obtained from long-time measurements of the MSD with the according values as obtained from a

short-time measurement of the dynamic structure factor and find good agreement. Owing to the high flexibility of scanned optical tweezers, one can also create channels with open ends which allow other particles to diffuse in and out. Such a situation is particularly interesting because it can serve as a model system for catalytic reactions in zeolitic materials, which are important for a number of chemical processes [23].

We acknowledge helpful discussions with Ralf Bubeck and Paul Leiderer. The work was financially supported by DFG (TR6).

-
- [1] V. Gupta, S.S. Nivarthi, A.V. McCormick, and H.T. Davis, *Chem. Phys. Lett.* **247**, 596 (1995).
 - [2] K. Hahn, J. Kärger, and V. Kukla, *Phys. Rev. Lett.* **76**, 2762 (1996).
 - [3] V. Kukla, J. Kornatowski, D. Demuth, I. Girnus, H. Pfeifer, L.V.C. Rees, S. Schunk, K. Unger, and J. Kärger, *Science* **272**, 702 (1996).
 - [4] D.G. Levitt, *Phys. Rev. A* **8**, 3050 (1973).
 - [5] J. Kärger, *Phys. Rev. A* **45**, 4173 (1992).
 - [6] T.E. Harris, *J. Appl. Probab.* **2**, 323 (1965).
 - [7] D. Jepsen, *J. Math. Phys. (N.Y.)* **6**, 405 (1965).
 - [8] H.v. Beijeren, K.W. Kehr, and R. Kutner, *Phys. Rev. B* **28**, 5711 (1983).
 - [9] M. Kollmann, *Phys. Rev. Lett.* **90**, 180602 (2003).
 - [10] J. Weitkamp, H. Kärger, H. Pfeifer, and W. Hölderich, *Zeolites and Related Microporous Materials: State of the Art* (Elsevier, Amsterdam, 1994).
 - [11] K. Hahn and J. Kärger, *J. Phys. Chem. B* **102**, 5766 (1998).
 - [12] H. Jobic, K. Hahn, J. Kärger, M. Bee, A. Tuel, M. Noack, I. Girnus, and G.J. Kearley, *J. Phys. Chem. B* **101**, 5834 (1997).
 - [13] R. Radhakrishnan and K.E. Gubbins, *Phys. Rev. Lett.* **79**, 2847 (1998).
 - [14] D.S. Sholl and K.A. Fichthorn, *Phys. Rev. Lett.* **79**, 3569 (1997).
 - [15] B. Lin, B. Cui, J.-H. Lee, and J. Yu, *Europhys. Lett.* **57**, 724 (2002).
 - [16] Q.-H. Wei, C. Bechinger, and P. Leiderer, *Science* **287**, 625 (2000).
 - [17] T. Palberg, W. Härtl, U. Wittig, H. Versmold, M. Würth, and E. Simnacher, *J. Phys. Chem.* **96**, 8180 (1992).
 - [18] A. Ashkin, J.M. Dziedzic, J.E. Bjorkholm, and S. Chu, *Opt. Lett.* **11**, 288 (1986).
 - [19] L.P. Faucheux, G. Stolovitzky, and A. Libchaber, *Phys. Rev. E* **51**, 5239 (1995).
 - [20] T.M. Squires and M.P. Brenner, *Phys. Rev. Lett.* **85**, 4976 (2000).
 - [21] G. Nägele, *Phys. Rep.* **272**, 215 (1996).
 - [22] B. Cui, H. Diamant, and B. Lin, *Phys. Rev. Lett.* **89**, 188302 (2003).
 - [23] Z. Karpinski, S.N. Gandhi, and W.M.H. Sachtler, *J. Catal.* **141**, 337 (1993).